

Imaging of NanoESI Spray Current with an Automated Digital Control Positioning System

Gary A. Valaskovic¹, Mike S. Lee²

¹New Objective, Inc., Woburn, MA, ¹Milestone Development Services, Newtown, PA

Introduction

Determination of nanospray emitter position for optimal signal intensity is often a trial-and-error process that involves adjustment of both emitter position and ESI high voltage. We have previously reported on the implementation of a feedback controlled nanoelectrospray source where either the spray voltage or nanospray emitter position is under feedback control (Valaskovic, et. al. JASMS, 2004, 15, 1201). Here we investigate the utility of a digital control system to map the spray current of the ESI plume for a variety of experimental conditions (flow rate, applied voltage, distance). Total and selected ion currents are generated via the systematic raster scanning of the nanospray emitter relative to the inlet and three dimensional maps are obtained.

Standard Digital PicoView[®] Acquire software was modified and combined with an additional scanning module to generate a raster scan pattern of the nanospray emitter with respect to the mass spectrometer inlet. Each movement to a given nanospray emitter X, Y, Z position triggered an MS acquisition and resulting data file. After conversion of these RAW-formatted files into the mzXML data format, a parsing and data visualization program was used to reconstruct the data into a mass filtered ion current image. Images were typically 2 x 2 mm with a pixel step size of 200 μm . The acquisition of a 100 point (10 x 10) data set was on the order of 30 minutes. The ion current resulting from a sample mixture of a singly-charged low molecular weight drug and a multiply charged peptide in aqueous-organic mobile phase delivered by continuous infusion was acquired.

Methods

Samples:

Continuous infusion experiments:

- Human angiotensin I, (Sigma-Aldrich[®]) and buspirone (Sigma-Aldrich[®]) was prepared in a final concentration of 1 μM and 200 nM respectively (30% ACN, 0.1% formic acid)

Continuous infusion pump & flow rate monitor:

- Syringe pump (Harvard Apparatus, PHD Model) with 250 μL glass Gastight Syringe (Hamilton[™])
- In-line digital flow rate monitor (Upchurch[®]); Target flow rate: 340 ± 20 nL/min.

Mass Spectrometer:

LCQ Deca[™] (Thermo Scientific)

- 3 Microscans/spectra
- Emitter-to-inlet distance: 0.25 to 4 mm (as stated in figures)
- ESI voltage: 1-4 kV (as stated in figures)
- Each image data point is from a 10 sec. RAW file acquisition

Digital PicoView[®] DPV-150 (New Objective) modified for scanned spray

- PicoView[®] Acquire[™] 1.51 with scanning module
- Raster scanning step size: 200 μm typical
- Image size: 10 x 10 pixels; 2 x 2 mm typical
- Self-pack PicoFrit[®] Emitter, 10 μm tip size (New Objective)

Data Analysis:

ReAdW software program (Institute for Systems Biology, <http://tools.proteomecenter.org/ReAdW.php>)

- Conversion of Thermo-generated RAW files to mzXML format

ViewImage (LabVIEW 8.2, National Instruments)

- Parses mzXML file and extracts mass spectrum
- Generates an image from multiple files

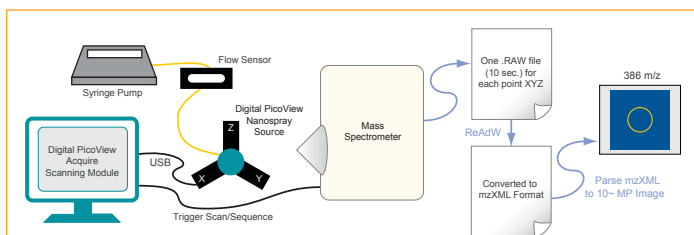


FIGURE 1 Schematic of the current mapping experiment. The nanospray emitter mounted on the XYZ stage of the source is scanned in front of the MS inlet in a raster pattern. The source generates a contact closure after every stage movement, triggering the acquisition a RAW file for that point. After a 100 point scan (10 x 10 image) the ReAdW program is used to convert files to the mzXML format. The ViewImage program loads the mzXML files for parsing and allows for the selection m/z range for image reconstruction. The orange circle in each map represents the size of the spectrometer inlet (≈ 0.5 mm).

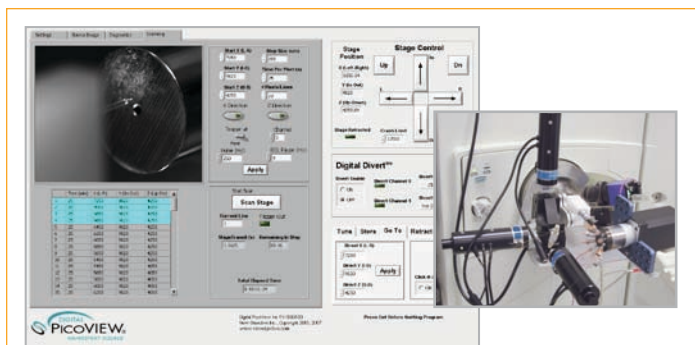


FIGURE 2 Screen shot of the prototype scan module within Digital PicoView® (right). The starting stage position, step size (μm), point dwell time, and number of points for the raster scan are all under user control.

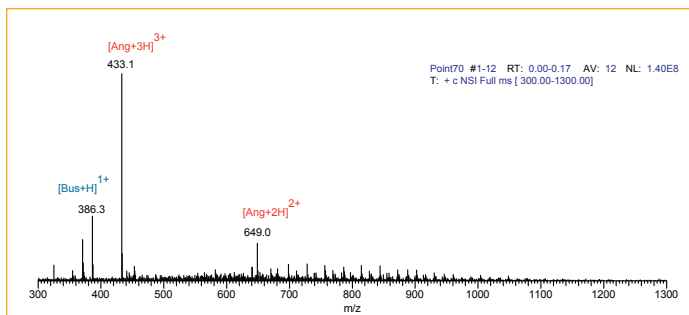
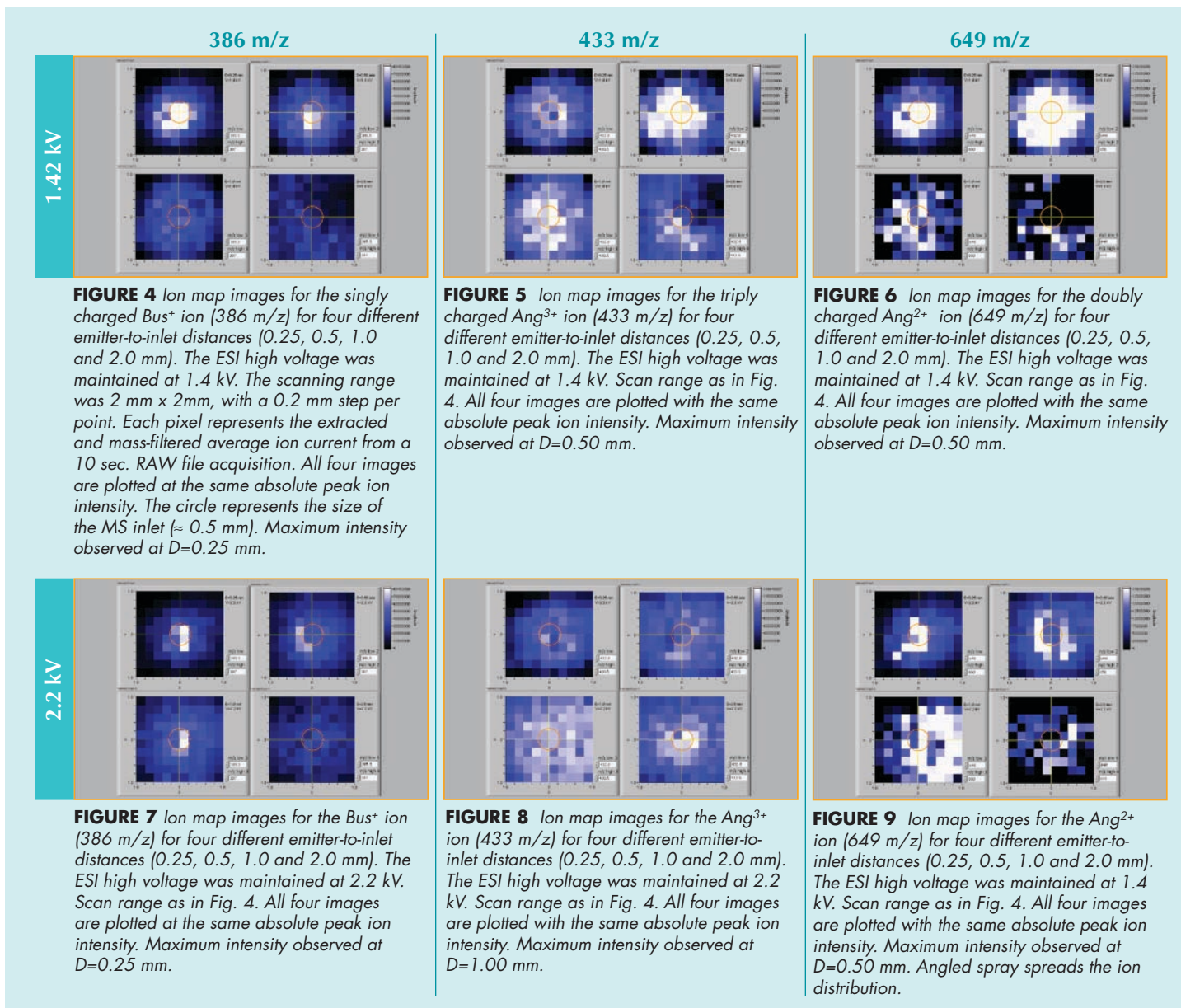


FIGURE 3 Representative full scan mass spectra for the sample mixture consisting of $1\ \mu\text{M}$ human angiotensin I (Ang) and $200\ \text{nM}$ buspirone (Bus) in 30% ACN, 0.1% formic acid. The doubly ($659\ \text{m/z}$) and triply ($433\ \text{m/z}$) charged ions for Ang and the singly charged ion ($386\ \text{m/z}$) for buspirone are prominent.



386 m/z

433 m/z

649 m/z

1.42 kV

FIGURE 4 Ion map images for the singly charged Bus^+ ion ($386\ \text{m/z}$) for four different emitter-to-inlet distances (0.25, 0.5, 1.0 and 2.0 mm). The ESI high voltage was maintained at 1.4 kV. The scanning range was $2\ \text{mm} \times 2\ \text{mm}$, with a $0.2\ \text{mm}$ step per point. Each pixel represents the extracted and mass-filtered average ion current from a 10 sec. RAW file acquisition. All four images are plotted at the same absolute peak ion intensity. The circle represents the size of the MS inlet ($\approx 0.5\ \text{mm}$). Maximum intensity observed at $D=0.25\ \text{mm}$.

FIGURE 5 Ion map images for the triply charged Ang^{3+} ion ($433\ \text{m/z}$) for four different emitter-to-inlet distances (0.25, 0.5, 1.0 and 2.0 mm). The ESI high voltage was maintained at 1.4 kV. Scan range as in Fig. 4. All four images are plotted with the same absolute peak ion intensity. Maximum intensity observed at $D=0.50\ \text{mm}$.

FIGURE 6 Ion map images for the doubly charged Ang^{2+} ion ($649\ \text{m/z}$) for four different emitter-to-inlet distances (0.25, 0.5, 1.0 and 2.0 mm). The ESI high voltage was maintained at 1.4 kV. Scan range as in Fig. 4. All four images are plotted with the same absolute peak ion intensity. Maximum intensity observed at $D=0.50\ \text{mm}$.

2.2 kV

FIGURE 7 Ion map images for the Bus^+ ion ($386\ \text{m/z}$) for four different emitter-to-inlet distances (0.25, 0.5, 1.0 and 2.0 mm). The ESI high voltage was maintained at 2.2 kV. Scan range as in Fig. 4. All four images are plotted at the same absolute peak ion intensity. Maximum intensity observed at $D=0.25\ \text{mm}$.

FIGURE 8 Ion map images for the Ang^{3+} ion ($433\ \text{m/z}$) for four different emitter-to-inlet distances (0.25, 0.5, 1.0 and 2.0 mm). The ESI high voltage was maintained at 2.2 kV. Scan range as in Fig. 4. All four images are plotted with the same absolute peak ion intensity. Maximum intensity observed at $D=1.00\ \text{mm}$.

FIGURE 9 Ion map images for the Ang^{2+} ion ($649\ \text{m/z}$) for four different emitter-to-inlet distances (0.25, 0.5, 1.0 and 2.0 mm). The ESI high voltage was maintained at 1.4 kV. Scan range as in Fig. 4. All four images are plotted with the same absolute peak ion intensity. Maximum intensity observed at $D=0.50\ \text{mm}$. Angled spray spreads the ion distribution.

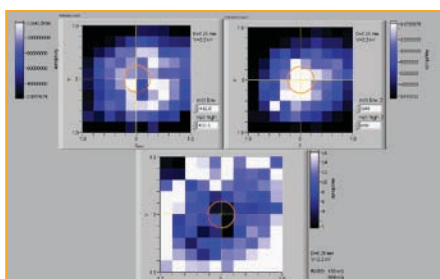


FIGURE 10 Ion map images of Ang^{3+} and Ang^{2+} (top row). Ratio of the two images (bottom row). ESI voltage was maintained at 2.2kV, inlet distance was 0.25 mm. Note the wider spatial distribution of the Ang^{3+} ions.

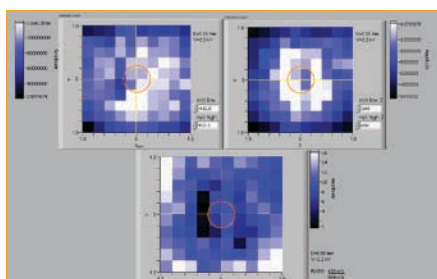


FIGURE 11 Ion map images of Ang^{3+} and Ang^{2+} (top row). Ratio of the two images (bottom row). ESI voltage was maintained at 2.2kV, inlet distance was 0.5 mm. The Ang^{3+} still shows a wider distribution than Ang^{2+} although it is less pronounced than in Figure 10.

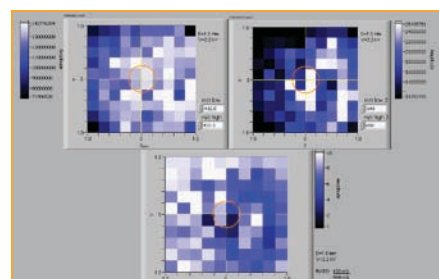


FIGURE 12 Ion map images of Ang^{3+} and Ang^{2+} (top row). Ratio of the two images (bottom row). ESI voltage was maintained at 2.2kV, inlet distance was 1.0 mm. The Ang^{3+} and Ang^{2+} ions show a similar distribution.

Working the Angles

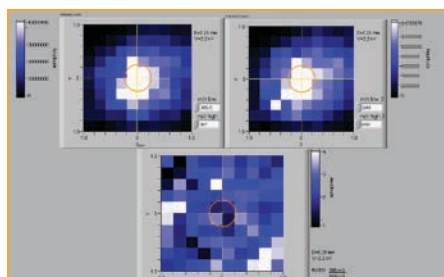


FIGURE 13 Ion map images of Bus^{1+} and Ang^{2+} (top row). Ratio of the two images (bottom row). ESI voltage was maintained at 2.2kV, inlet distance was 0.25 mm. The Bus^{1+} and Ang^{2+} ions show a distinctly similar distribution.

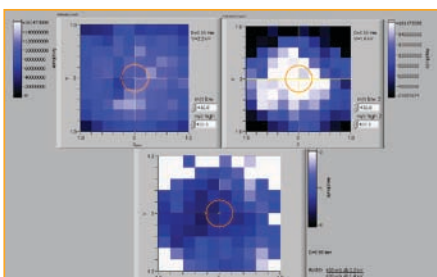


FIGURE 14 Ion map images of Ang^{3+} for two different ESI voltages (2.2 and 1.4 kV, top row). Ratio of the two images (bottom row). Inlet distance was 0.5 mm. Note the wider spatial distribution for the 2.2 kV setting.

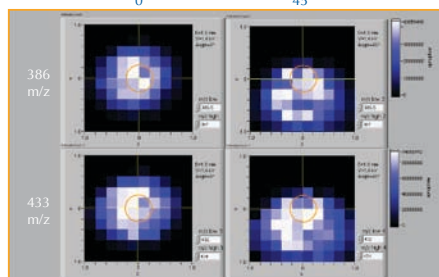
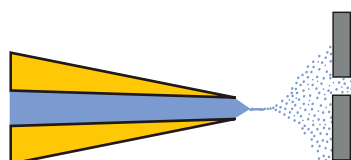


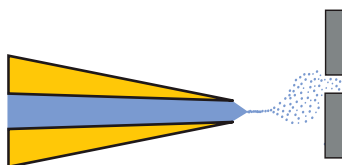
FIGURE 15 Ion map images for normal (left column, 0° spray angle, i.e. straight in, on-axis) and angled spray (right column, 45° spray angle). The ESI high voltage was maintained at 1.4 kV. The scanning range was 2 mm x 2 mm, with a 0.2 mm step per point. The top row images are for Bus^+ , the bottom row Ang^{3+} .

Imaging Case (i): Mapping of ion current within the plume



Inlet gas flow does not perturb the spray plume.
Passive droplet/cluster sampling

Imaging Case (ii): Mapping of ion current convolved with droplet collection



Inlet gas flow perturbs the spray plume.
Active droplet/cluster sampling

Two possible cases for ion mapping experiments:

In case (i) the gas flow into the inlet vacuum system is not sufficient to disturb the spatial distribution of droplets in the spray plume. Ion maps generated for case (i) represent the natural distribution of ion-generating droplets within the plume.

In case (ii) the gas flow into the inlet is sufficient to disturb plume distribution. An ion maps generated for case (ii) is a convolution of the ion-generating droplet distribution within the plume and the droplet-capture function of the inlet. Orthogonal spray imaging (not shown) confirms that case (ii) holds for conventional nanospray operation.

Conclusions

- A singly charged (basic) drug molecule (MW=385) demonstrated a simple Gaussian-like ion distribution (X, Y), having a maximum ion intensity with the emitter in close proximity to the inlet (0.25 mm)
- The distribution of Bus⁺ ion was similar for low (1.4 kV) and high (2.2 kV) voltage settings
- A multiply charged peptide (MW=1296) showed a more complex distribution. Surprisingly the doubly and triply charged ions showed marked differences in distribution:
 - The doubly charged Ang²⁺ ion (649 m/z) showed a simple distribution, with a maximum intensity at an inlet distance of 0.5 mm.
 - The triply charged Ang³⁺ ion had a broader (X, Y) ion distribution, with a maximum intensity at an inlet distance of 1.0 mm.
- The distribution (X, Y) of Ang³⁺ was broadest at higher voltage settings
- Distribution (X, Y) differences between Ang³⁺ and Ang²⁺ were the greatest at high voltage (2.2 kV) and close inlet proximity (0.25 mm)
- The distribution (X, Y) of Bus⁺ and Ang²⁺ was substantially similar
- Changing the spray angle from 0° (normal) to 45° broadened the ion map distribution for all observed ions.
- Operating the nanospray emitter at larger distances (≥ 2 mm) from the inlet eases positional dependence of signal at the sacrifice of maximum ion current
- Using a close nanospray emitter-to-inlet position with operation at a higher than normal voltage might be useful as a means to aid in the discrimination of peptides having a charge of 3+ or greater